Korean J. Chem. Eng., 37(6), 1086-1096 (2020)
DOI: 10.1007/s11814-020-0518-1

pISSN: 0256-1115
eISSN: 1975-7220

Formation of calcium carbonates from $Ca(OH)_2$-H_2O-supercritical CO_2 using a rapid spraying method

Jin-Seok Kim and Ho Young Jo†

Department of Earth and Environmental Sciences, Korea University, 145 Anam-ro, Seongbuk-gu, Seoul 02841, Korea
(*Received 11 November 2019 • accepted 19 February 2020*)

Abstract−Particle formation techniques using supercritical fluid are simple processes that can control particle size and morphology, although high-pressure is required. The purpose of this study was to investigate how the experimental conditions affect the extent and rate of $CaCO_3$ conversion and the size and morphology of the precipitated $CaCO_3$ from the carbonation tests with rapid spraying of reactants causing rapid depressurization of supercritical fluid. The relatively low temperature and pressure conditions (35 °C and 7.5 MPa) resulted in low $CaCO_3$ conversion efficiency (41.4-51.9%), high vaterite content (70-78%) of $CaCO_3$, and smaller-sized particles. The relatively high temperature and pressure conditions (80 °C and 12.0 MPa) resulted in high $CaCO_3$ conversion efficiency (66.8-73.2%), high calcite content (50-80%) of $CaCO_3$, and larger-sized particles. The particle size of solid products ranged between 20 and 180 nm with approximately a peak of 100 nm in the particle size distribution (PSD) curve, irrespective of the test conditions; however, shorter reaction times led to smaller particles. The optimal conditions under which the extent of $CaCO_3$ conversion and calcite content were maximum were 50 °C, 9.0 MPa, and 1 h of reaction time ($CaCO_3$ conversion: 92.9%; calcite content of $CaCO_3$: 87%).

Keywords: Carbon Capture, Carbon Utilization, Crystallisation, Precipitation, Supercritical Fluids

INTRODUCTION

Particulate calcium carbonate ($CaCO_3$) is widely used as a filler, pigment, or additive in various industries (e.g., paper, paint, coatings, plastics, sealants, cosmetics, pharmaceutics, and cement). Particulate $CaCO_3$ is obtained by grinding natural calcium carbonate, resulting in ground calcium carbonate (GCC), or by inducing precipitation through a chemical reaction, resulting in precipitated calcium carbonate (PCC). PCC is more widely used than GCC because $CaCO_3$ with a small particle size and variable morphology can be obtained through modulation of the reaction conditions [1,2]. $CaCO_3$ has three polymorphs: calcite, aragonite, and vaterite. Calcite, which is rhombohedral-scalenohedral shaped, is the most stable polymorph under atmospheric conditions and is well formed at high pH and low temperatures. Aragonite is needle-shaped and metastable under ambient temperature and high-pressure conditions. Vaterite, which is spherical, is the meta-form of calcite and aragonite and is the least stable phase among the three polymorphs. As the reaction continues, relatively unstable aragonite and vaterite recrystallize and transform into stable calcite [3-5].

Industrially, PCC is conventionally produced by bubbling carbon dioxide (CO_2) gas through a calcium hydroxide ($Ca(OH)_2$) slurry. The overall equation for the PCC formation is

$$Ca(OH)_2+CO_2\rightarrow CaCO_3+H_2O \quad (1)$$

The extent and rate of PCC conversion in the conventional PCC production processes depend on the extent and rate of dissolution of $Ca(OH)_2$ and CO_2 gas in water. $Ca(OH)_2$ is partially soluble in water. Dissolved Ca^{2+} ions react with CO_3^{2-} ions produced by the dissolution of CO_2 gas into water, leading to precipitation of $CaCO_3$. However, $CaCO_3$ can be initially precipitated on the surface of $Ca(OH)_2$ particles, resulting in no further dissolution of $Ca(OH)_2$ and no further formation of $CaCO_3$. The formation of $CaCO_3$ surrounding $Ca(OH)_2$ particles leads to a low extent of $CaCO_3$ conversion [6,7]. Accordingly, the conventional PCC production processes using a $Ca(OH)_2$ slurry and CO_2 gas are relatively slow and their $CaCO_3$ conversion rate is low. As a result, high energy and production costs are needed to achieve a high degree of $CaCO_3$ conversion [8,9].

Supercritical fluids (SCFs), with their relatively low viscosity and high diffusivity, have been extensively used for particle formation, especially in the pharmaceutical, nutrient, cosmetic, and chemical industries. Particle formation techniques using SCFs are simple processes that can control particle size and morphology, even though high-pressure operation is problematic [10]. Supercritical CO_2 (SC CO_2) has been proposed as a reactant to enhance the extent and rate of PCC production because SC CO_2 can induce a high partial CO_2 pressure in water, resulting in a high concentration of CO_2 dissolved in water. The SC CO_2 phase, which occurs at temperatures and pressures greater than 31 °C and 7.38 MPa, respectively, exhibits intermediate properties between those of a liquid and a gas [11]. Montes-Hernandez et al. [9] reported that 50.7 and 93.7% of $CaCO_3$ conversion were obtained in 15 min and 4 h, respectively, when a $Ca(OH)_2$ slurry and SC CO_2 were reacted at 90 °C and 9 MPa. Regnault et al. [12] also reported that complete $CaCO_3$ conversion occurred within 2 h in a carbonation test of a $Ca(OH)_2$ slurry

†To whom correspondence should be addressed.
E-mail: hyjo@korea.ac.kr

and SC CO_2 at 80-200 °C and 16 MPa.

However, the carbonation method with SC CO_2 still has problems with respect to $CaCO_3$ precipitation on the $Ca(OH)_2$ surface. The carbonation of a $Ca(OH)_2$ slurry using SC CO_2 in combination with ultrasonic agitation has been proposed to reduce the effect of $CaCO_3$ precipitation on the $Ca(OH)_2$ surface [7,13]. López-Periago et al. [7,13] proposed a novel method for carbonating $Ca(OH)_2$ slurry using SC CO_2 combined with ultrasonic agitation to enhance the extent and rate of $CaCO_3$ conversion by promoting mass transfer through the initially precipitated $CaCO_3$ layers on the $Ca(OH)_2$ surface. They reported that 88% conversion after 1 h using $Ca(OH)_2$ and 99% conversion after 1 h using CaO was achieved when a SC-CO_2 system combined with ultrasonic agitation was used.

Unlike the method of producing $CaCO_3$ via interaction between SC CO_2 and Ca-bearing materials in a reactor with the aid of ultrasonic agitation, Hawae et al. [14] synthesized nano-sized $CaCO_3$ via rapid expansion of supercritical solution (RESS) method using SC CO_2. The RESS method has been used to produce nanoscale to microscale particles by dissolving solute into an SCF and rapidly decreasing the SCF pressure through a fine nozzle to atmospheric pressure [10]. Hawae et al. [14] reacted $Ca(OH)_2$ solution with SC CO_2 in a reactor under 50 °C and 10 or 15 MPa conditions for 30 min. Afterwards, $CaCO_3$ particles with average sizes of 93 and 229 nm at 10 and 15 MPa, respectively, were obtained by rapidly spraying the mixture into a container through a nozzle. Hawae et al. [14] only reported particle sizes and scanning electron microscopy (SEM) images of the solid products obtained under conditions of 50 °C and 10 or 15 MPa for 30 min. The RESS method produces small particles with narrow size distribution; however, the particle morphology and size distribution can be varied through manipulation of the test conditions (e.g., temperature, pressure, and reaction time). However, studies on $CaCO_3$ formation by the RESS method under various test conditions are very rare.

In the present study, the carbonation characteristics of $Ca(OH)_2$-H_2O-SC CO_2 using a rapid spraying method under various test conditions were investigated. The purpose of this study was to evaluate how the experimental conditions affect the extent and rate of $CaCO_3$ conversion and the size and morphology of the precipitated $CaCO_3$. The carbonation tests were conducted on $Ca(OH)_2$-H_2O slurry with SC CO_2 combined with a rapid spraying method (i.e., rapid spraying reactants within ca. 5 s through a small-diameter tube into a plastic container inducing rapid depressurization), which is similar to the RESS method, under various test conditions (35 °C and 7.5 MPa, 50 °C and 9.0 MPa, and 80 °C and 12.0 MPa) for various reaction times (0.5, 1.0, 2.5, and 4.0 h). The $CaCO_3$ content of the solid products, the polymorph fractions of $CaCO_3$, and the particle size and morphology of the solid products were characterized.

EXPERIMENTAL

1. Carbonation Tests using SC CO_2 Combined with a Rapid Spraying Method

Analytical-reagent-grade $Ca(OH)_2$ (Sigma-Aldrich, Darmstadt,

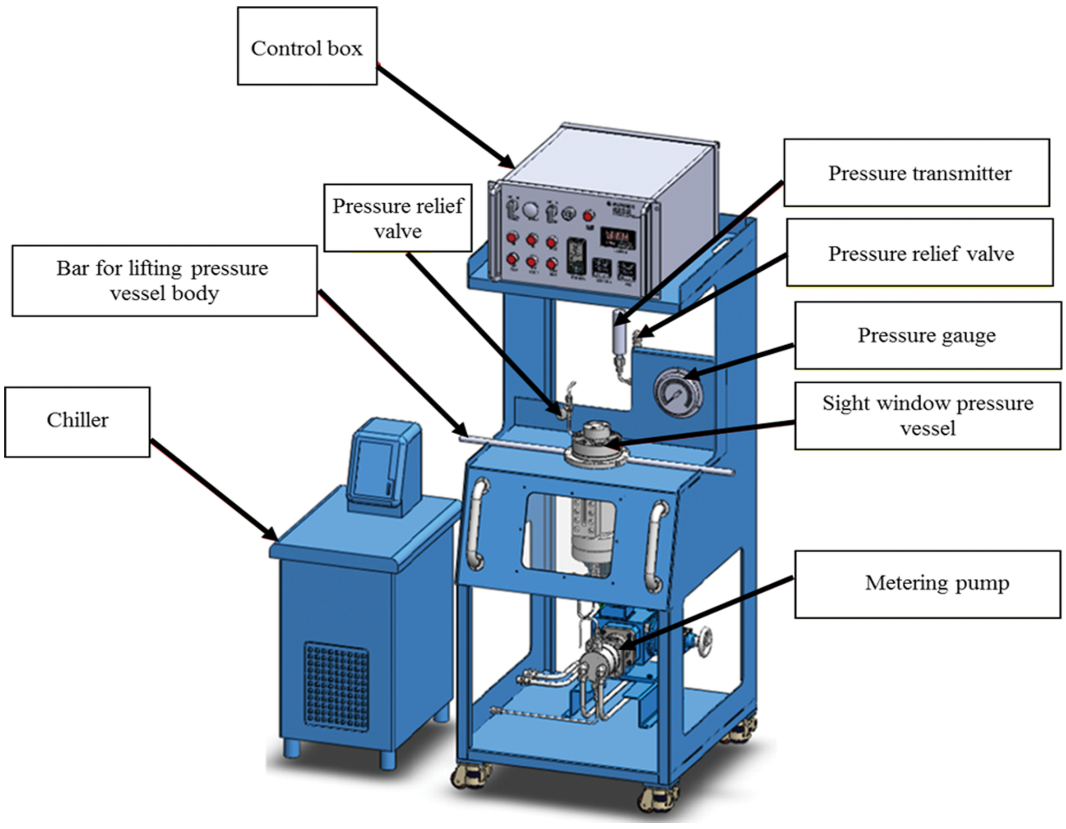

Fig. 1. Schematic of high-pressure chamber system (HPCS).

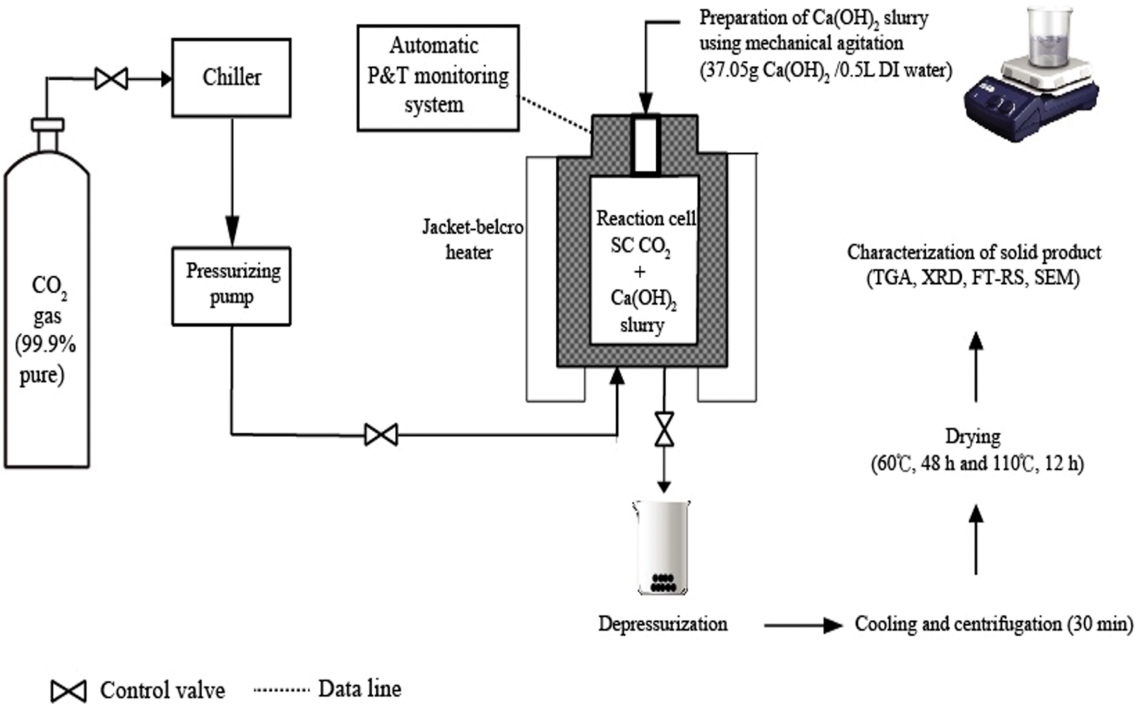

Fig. 2. Schematic of the carbonation test setup using HPCS.

Germany: 96% purity) was used as a Ca source for carbonation tests. CO_2 gas (Seoul Special Gas Co., Seoul, South Korea: 99.99% purity) was used in this study. The carbonation tests were conducted on H_2O-$Ca(OH)_2$-SC CO_2 slurry at elevated temperature and pressure conditions in a batch reactor combined with the rapid spraying method to produce micro-sized $CaCO_3$. The supercritical solution was rapidly depressurized through a small tube to atmospheric pressure, which could cause sudden volume expansion of the supercritical solution like the RESS method that is used a fine nozzle for spraying the H_2O-$Ca(OH)_2$-SC CO_2 slurry. A schematic of the carbonation test is shown in Fig. 1. The mixture of 37.05 g of the analytical-reagent-grade $Ca(OH)_2$ and 0.5 L of deionized (DI) water [i.e., 1 mol/L $Ca(OH)_2$] was placed in a high-pressure stainless steel chamber (HPSC, 750 mL, Phosentech, Inc., Daejeon, Korea) (Fig. 1). The tests were conducted under different temperature and pressure conditions of 35-80 °C and 7.5-12.0 MPa, which satisfy the conditions for SC-CO_2 (i.e., >31 °C and >7.38 MPa) [15], for various test periods (0.5-4 h) to investigate how the different test conditions affect the extent and rate of $CaCO_3$ conversion and the size and morphology of the formed $CaCO_3$.

The HPSC was heated with a jacket-velcro heater to the target temperature (35, 50, or 80 °C) immediately after the $Ca(OH)_2$ slurry was placed into the HPSC. When the target temperature was reached, 99.99% pure CO_2 gas was injected into the HPSC and pressurized to the target pressure (7.5, 9.0, or 12.0 MPa) using a syringe pump while the system was maintained at the target temperature. The carbonation tests were conducted under three test conditions: 35 °C and 7.5 MPa, 50 °C and 9.0 MPa, and 80 °C and 12.0 MPa. The test conducted under each test condition was terminated at the designated time (0.5, 1.0, 2.5, or 4.0 h).

After the designated reaction time was reached, the $Ca(OH)_2$ slurry that had reacted with SC CO_2 in the HPSC was rapidly sprayed (within ca. 5 s) through a small-diameter tube with an inner diameter of 1.5 mm into a plastic container to induce rapid depressurization. As a result, the pressure of the mixture of SC CO_2 and $Ca(OH)_2$ slurry decreased dramatically, leading to extremely supersaturated conditions. The extreme supersaturation can induce crystallization via rapid nucleation of $CaCO_3$ [16]. After the $Ca(OH)_2$ slurry that reacted with SC CO_2 in the HPSC was completely sprayed from the HPSC into a plastic container, the solid and liquid in the plastic container were separated by centrifugation at 4,000 revolutions per minute (rpm) for 30 min for subsequent characterization of the solid product. After centrifugation, the solid was dried in an oven at 60 °C for 48 h and consecutively at 110 °C for 12 h to completely eliminate adsorbed water (Fig. 2).

2. Characterization of Solid Products

Dried solid was ground and passed through a #100 sieve (<0.15 mm). The $CaCO_3$ content of the dried solid products obtained after the carbonation tests was determined by thermogravimetric analysis (TGA, TGA 2050, TA Instruments, New Castle, Delaware) at the Korea Institute of Science and Technology in Seoul, Korea. The dried solid products were heated to 800 °C at 10 °C/min under an air flow rate of 100 mL/min. The $CaCO_3$ content was estimated using the following equation suggested by Pane and Hansen [17]:

$$W_{CaCO_3}(wt\%) = (W_{600} - W_{780}) \times \frac{MW_{CaCO_3}}{MW_{CO_2}} \quad (2)$$

where W_{CaCO_3} represents the weight percent of $CaCO_3$ in the solid product, W_{600} and W_{780} represent the weight percent of the remaining solid products at 600 and 780 °C, respectively, and MW_{CaCO_3} (100.09 g/mol) and MW_{CO_2} (44.01 g/mol) represent the molecular weights of $CaCO_3$ and CO_2, respectively.

The relative amounts of the $CaCO_3$ polymorphs of the dried solid products obtained after the carbonation test were estimated by Fourier transform raman spectrometry (FT-RS, LabRam ARAMIS IR2, Horiba, Kyoto, Japan). The excitation source was a diode laser operating at 532 nm with a power of approximately 50 mW. Although X-ray diffraction (XRD) and FT-RS can be used to estimate the relative amounts of the $CaCO_3$ polymorphs in carbonate materials, Kontoyannis and Vagenas [18] suggested that FT-RS exhibits advantages over XRD in this application. Accordingly, we used the FT-RS analysis results for the solid products to estimate the relative fraction of the $CaCO_3$ polymorphs according to the equation suggested by Kontoyannis and Vagenas [28] without obtaining the calibration data:

$$X_A = \frac{1.395 \times I_{700}}{I_{711} + 1.395 \times I_{700} + 9.30 \times I_{750}} \quad (3)$$

$$X_C = \frac{I_{711} \times X_A}{1.395 \times I_{700}} \quad (4)$$

$$X_V = 1.0 - X_A - X_C \quad (5)$$

where X_A, X_C, and X_V are the relative fractions (%) of aragonite, calcite, and vaterite, respectively, I represents the intensity of the excitation laser line, and subscripts of 700, 711, and 750 denote the wavenumber of the Raman shift. Many researchers reported the relative composition of polymorphs of synthesized $CaCO_3$ calculated using the empirical equation proposed by Kotoyannis and Vegenas [18] without providing calibration data [19-28]. However, the calibration data for quantification of polymorphs' composition in the $CaCO_3$ using the FT-RS analysis can be required to obtain better results of the quantification.

The morphology of the dried solid products was analyzed by field-emission scanning electron microscopy (FE-SEM, Hitachi S-4300, Tokyo, Japan) at the Green Manufacturing Research Center in Seoul, Korea to investigate how the test conditions affect the particles' surface morphology and particle size distribution (PSD). The dried solid powder was sprayed onto carbon tape and coated with platinum for SEM analysis. The PSD of solid particles was obtained by analyzing SEM images using the Image J software. The Feret diameters of the particles were extracted from two or more SEM images for application to various polymorphs with different shapes. The Feret diameter is the distance between two parallel tangents that touch the outline of a randomly oriented particle. This value, also called the calliper diameter, depends on the particle orientation [29,30]. The PSD of the emulsion obtained after carbonation tests was also determined using a particle size analyzer (dynamic light scattering, Zetasizer Nano ZS, Malvern Panalytical Ltd., Malvern, United Kingdom) at the National Nanofab Center in Seoul. The results of the particle size analysis of the emulsion were compared with those obtained by SEM image analysis of dried solid products using the Image J software.

RESULTS AND DISCUSSION

1. $CaCO_3$ Content of Solid Products

TGA of the unreacted $Ca(OH)_2$ and solid products obtained from the carbonation tests using the spraying method was conducted to estimate the $CaCO_3$ content of the solid products. The TGA results for the unreacted $Ca(OH)_2$ and solid products obtained under different conditions are shown in Fig. 3. Dehydroxylation of $Ca(OH)_2$ and decomposition of $CaCO_3$ occur at approximately at 420-460 °C and 600-800 °C, respectively [31,32]. A substantial mass loss of the unreacted $Ca(OH)_2$ was observed between 380 and 460 °C, whereas the solid products exhibited a large mass loss between 600 and 800 °C (Fig. 3), indicating that the unreacted $Ca(OH)_2$ and solid products were mostly composed of $Ca(OH)_2$ and $CaCO_3$, respectively. However, the magnitude of the mass losses in the ranges between 380-460 °C and 600-800 °C varied depending on the test conditions (i.e., temperature, pressure, and reaction time), suggesting that the extent of conversion of $Ca(OH)_2$ to $CaCO_3$ was depen-

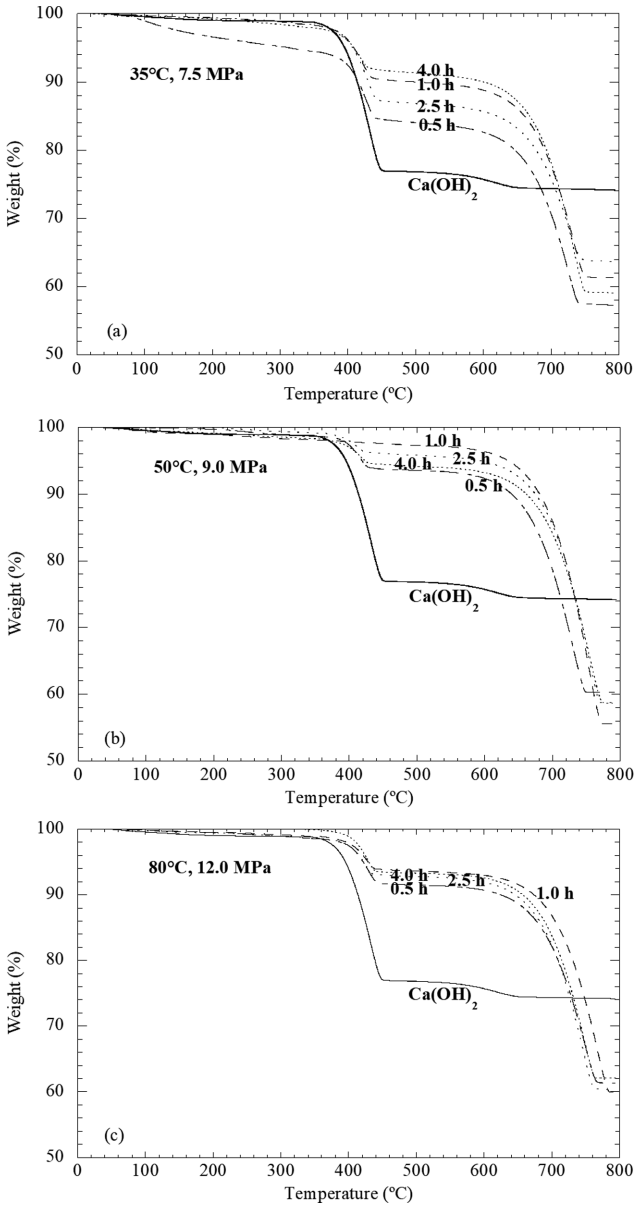

Fig. 3. TGA results for the solid products obtained from carbonation tests at (a) 35 °C and 7.5 MPa, (b) 50 °C and 9 MPa, and (c) 80 °C and 12 MPa.

Table 1. TGA results and calculated content of solid products obtained from carbonation tests

Carbonation test conditions			TGA results			$CaCO_3$ content (%)
Temperature (°C)	Pressure (MPa)	Reaction time (h)	W_{600}[a] (%)	W_{780}[b] (%)	Weight loss (%)	
35	7.5	0.5	82.6	57.3	25.3	47.7
		1.0	88.8	61.3	27.5	51.9
		2.5	85.7	63.7	21.9	41.4
		4.0	90.0	59.1	30.9	58.3
50	9.0	0.5	92.4	60.3	32.1	73.0
		1.0	96.4	55.5	40.8	92.9
		2.5	94.9	58.7	36.1	82.2
		4.0	93.2	58.7	34.6	78.7
80	12.0	0.5	90.7	61.4	29.4	66.8
		1.0	93.0	61.0	31.9	73.2
		2.5	91.9	60.4	31.5	71.7
		4.0	92.6	62.1	30.5	69.4

[a]Weigth percent of the remaining solid product at 600 °C.
[b]Weigth percent of the remaining solid product at 780 °C.

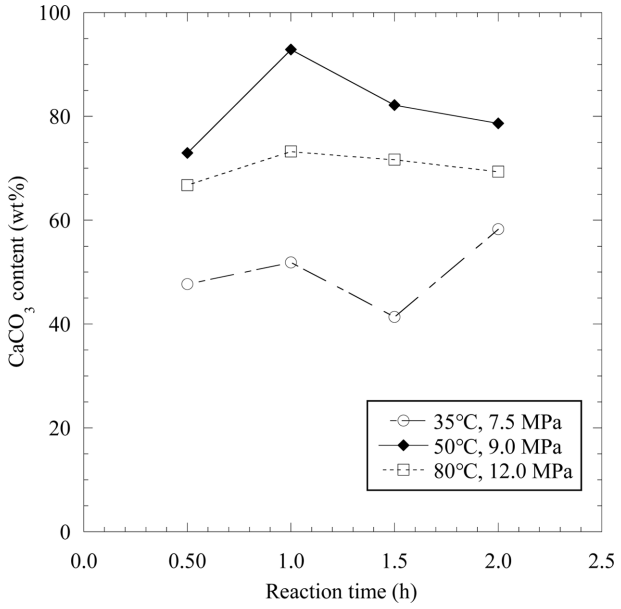

Fig. 4. $CaCO_3$ content of the solid products obtained from carbonation tests under various conditions, as determined from TGA results.

dent on the test conditions.

The $CaCO_3$ content of the solid products obtained under various test conditions, as estimated using Eq. (1), is shown in Table 1 and Fig. 4. The $CaCO_3$ content was relatively low in the solid product obtained at 35 °C and 7.5 MPa (41.4-51.9%) but was relatively high in the product obtained at 50 °C and 9.0 MPa (73.0-92.9%) for a given reaction time. These results indicate that the extent of $CaCO_3$ conversion at 35 °C and 7.5 MPa was low, whereas that at 50 °C and 9.0 MPa was high. Vance et al. [32] conducted carbonation tests by reacting $Ca(OH)_2$ with liquid CO_2 or SC CO_2 at various temperatures (8-42 °C) and pressures (6-10 MPa). They reported that although the pressure and temperature had little influence on the extent of $CaCO_3$ conversion, the extent of conversion was slightly higher in $Ca(OH)_2$ reacted with SC CO_2 than in $Ca(OH)_2$ reacted with liquid CO_2. In the present study, the extent of $CaCO_3$ conversion under a specific set of conditions (50 °C and 9.0 MPa) was large, suggesting that optimum conditions exist for the carbonation of $Ca(OH)_2$ using SC CO_2 combined with the rapid spraying method. Unlike the conventional carbonation method with SC CO_2, in the present study, $Ca(OH)_2$ slurry was reacted with SC CO_2 and the pressure was rapidly decreased (i.e., within ca. 5 s) when the mixture was sprayed into a plastic container through a very small-diameter (1.5 mm) tube, inducing rapid expansion of the mixture of reacted $Ca(OH)_2$ slurry and SC CO_2 by rapid depressurization.

The highest $CaCO_3$ content (51.9-92.9%) was obtained at reaction time of 1.0 h, regardless of test conditions. For example, 92.9% of the $CaCO_3$ content was obtained at 1.0 h, however decreasing to 78.7% after 4.0 h under conditions of 50 °C and 9.0 MPa. Similarly, the $CaCO_3$ content substantially increased to 66.8% at 0.5 h, reached a maximum (73.2%) at 1.0 h, and decreased to 69.4% at 4.0 h under conditions of 80 °C and 12.0 MPa (Table 1 and Fig. 4). By contrast, Montes-Hernandez et al. [9] reported $CaCO_3$ conversion of 50.7% at 15 min and 93.7% at 4 h when $Ca(OH)_2$ slurry was reacted with SC CO_2 at 90 °C and 9.0 MPa, and the $CaCO_3$ conversion gradually increased with increasing reaction time when the pressure was gradually decreased. Vance et al. [32] also reported that the extent of $CaCO_3$ conversion when $Ca(OH)_2$ was reacted with liquid CO_2 at 25 °C and 8.0 MPa substantially increased to approximately 70% at 0.5 h and thereafter gradually increased to 80% at 2.0 h. Vance et al. [32] attributed the promotion of $CaCO_3$ conversion to the small volume expansion of $CaCO_3$ crystals associated with the carbonation of $Ca(OH)_2$, which causes exfoliation of initially formed $CaCO_3$ layers onto the $Ca(OH)_2$ surface. The exfoliation leads to easy penetration of CO_2 into the reactive surface of unreacted $Ca(OH)_2$, resulting in further carbonation under

the high pressure condition. Vance et al. [32] decompressed the reactor by gently releasing CO_2 from the reactor at the end of reaction (i.e., carbonation). On the other hand, in the present study, the exfoliation of initially formed $CaCO_3$ layers could be significantly promoted by rapid spraying, which induced rapid depressurization, as soon as the reaction was completed in the reactor, which caused rapid expansion of the precipitated $CaCO_3$ crystals. The $CaCO_3$ layers formed on the $Ca(OH)_2$ surface after 1 h of reaction can be easily exfoliated, which is shorter than the optimal time (~2.0 h) reported by Vance et al. [32], because of their relatively small thickness resulting from the short reaction period. However, exfoliation of the $CaCO_3$ layers formed on the $Ca(OH)_2$ surface during reactions conducted for longer than 1 h can be difficult because the $CaCO_3$ layers are thicker. Further study might be needed to validate this hypothesis.

2. $CaCO_3$ Polymorph Content of Solid Products

The FT-RS results used to estimate the relative amounts of the $CaCO_3$ polymorphs are shown in Fig. 5. The Raman peaks used to analyze the amounts of portlandite [$Ca(OH)_2$], calcite, aragonite, and vaterite are typically those at approximately 360, 711, 700, and 750 cm^{-1}, respectively [28,33]. The portlandite peak in the spectrum of the solid products obtained at 35 °C and 7.5 MPa was more intense than those in the spectra of the solid products obtained at 50 °C and 9.0 MPa and 80 °C and 12.0 MPa; however, the peaks of the carbonate polymorphs in the spectra of the solid products obtained at 35 °C and 7.5 MPa were lower than those of the solid prod-

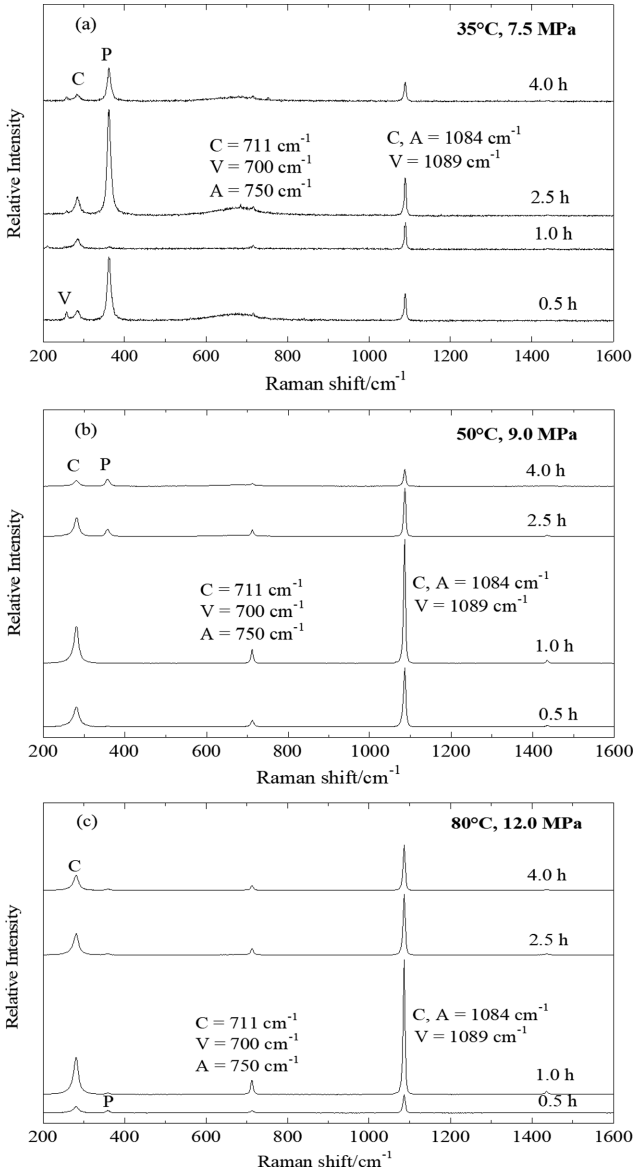

Fig. 5. Raman spectra of the solid products obtained from carbonation tests under conditions of (a) 35 °C and 7.5 MPa, (b) 50 °C and 9 MPa, and (c) 80 °C and 12 MPa. A: aragonite, C: calcite, P: portlandite ($Ca(OH)_2$), V: vaterite.

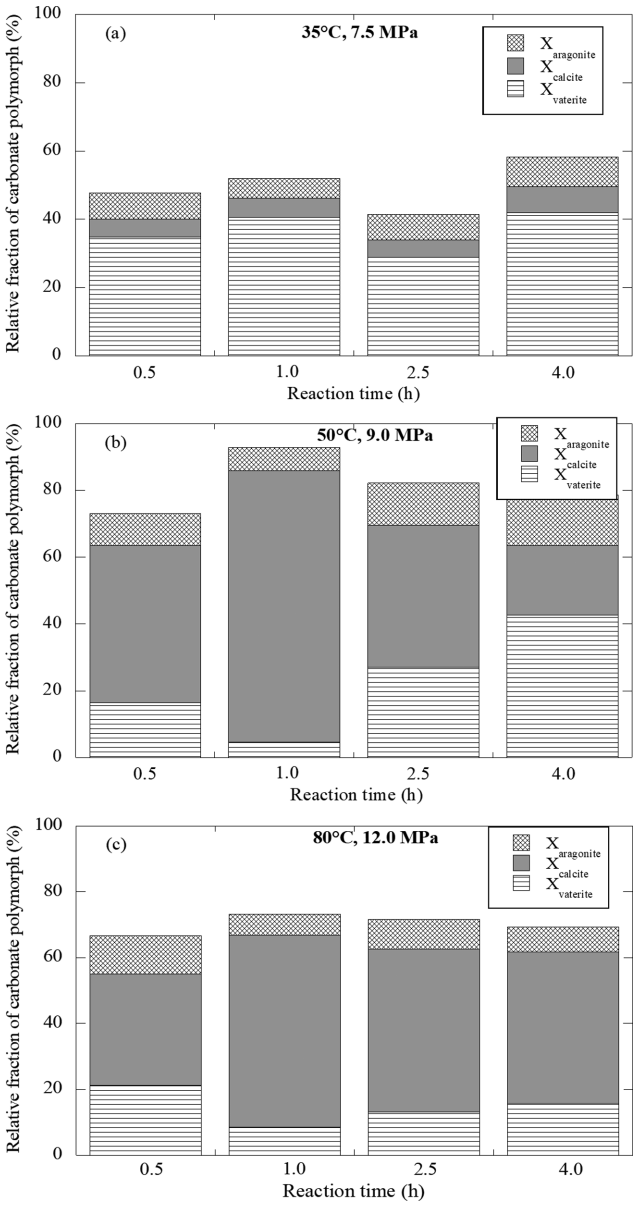

Fig. 6. Relative fractions of $CaCO_3$ polymorphs in solid products obtained from carbonation tests. $X_{aragonite}$: aragonite fraction, $X_{calcite}$: calcite fraction, and $X_{vaterite}$: vaterite fraction.

ucts obtained at 50 °C and 9.0 MPa and 80 °C and 12.0 MPa (Fig. 5). These results indicate that the extent of $CaCO_3$ conversion at 35 °C and 7.5 MPa was greater than that under the other investigated temperature and pressure conditions. The peaks of the carbonate polymorphs were most intense in the spectra of the solid products reacted for 1.0 h at both 50 °C, 9.0 MPa and 80 °C, 12.0 MPa. These FT-RS results are consistent with the TGA results shown in Fig. 3.

The carbonate polymorph fractions of $CaCO_3$ were estimated using the FT-RS results in conjunction with Eqs. (2)-(4). The amount of amorphous $CaCO_3$ in the synthesized $CaCO_3$ was found to be relatively small when the results of FT-RS analysis on the synthesized $CaCO_3$ were compared to those reported by Harris et al. [34]. In addition, many studies used the empirical equations proposed by Kotoyannis and Vegenas [18] for quantifying the composition of polymorphs in synthesized $CaCO_3$ using results of FT-RS analysis [19-28]. Although they mentioned amorphous $CaCO_3$ formation at the early stage of synthesis, the quantity of amorphous $CaCO_3$ was ignored from quantitative calculations. Thus, the quantity of amorphous $CaCO_3$ was ignored in the quantitative calculation in the present study.

The estimated carbonate polymorph fractions of $CaCO_3$ obtained under various test conditions are shown in Table 2. In addition, the carbonate polymorph fractions of solid products obtained under various test conditions were estimated using both the TGA and FT-RS results. Fig. 6 shows the carbonate polymorph fractions of solid products obtained using both the TGA and FT-RS results as a function of the reaction time. Vaterite was the dominant $CaCO_3$ polymorph (30-41%) in the solid products obtained at 30 °C and 7.5 MPa. The vaterite content increased with decreasing temperature from 80 to 35 °C (Fig. 6). Vaterite preferentially precipitates under supersaturation conditions with respect to Ca^{2+} and CO_3^{2-} ions [35,36]. The pressures (7.5-12.5 MPa) used in this study are likely sufficiently high to form vaterite, causing a high CO_2 partial pressure. However, the decrease in temperature from 80 to 35 °C can cause an increase in CO_2 dissolution in $Ca(OH)_2$ solution. In addition, the solubility of $Ca(OH)_2$ increases with decreasing temperature from 80 to 35 °C. This high dissolution of CO_2 and $Ca(OH)_2$ in the solution under low-temperature conditions (30 °C and 7.5 MPa) causes supersaturation with respect to Ca^{2+} and CO_3^{2-} ions, leading to a high vaterite content. As a result, vaterite is preferentially formed under the low-temperature conditions (30 °C and 7.5 MPa).

The calcite content of the solid products tended to increase with increasing temperature and pressure, becoming the dominant polymorph of $CaCO_3$ in the solid products obtained at 50 °C and 9.0 MPa (Fig. 6). The calcite content was relatively high in the $CaCO_3$ reacted with SC CO_2 at 50 °C and 9.0 MPa (87%) and at 80 °C and 12.0 MPa (80%) for 1 h (Table 2). An increase in the temperature under the high-pressure conditions (9.0 and 12.0 MPa) can lead to a decrease in dissolution of CO_2 and $Ca(OH)_2$ in the solution, resulting in lower concentrations of supersaturated Ca^{2+} and CO_3^{2-} ions. In particular, changes in the calcite content of the $CaCO_3$ in the solid products obtained at 80 °C and 12.0 MPa with increasing reaction time were relatively small (Fig. 6). These results suggest that the $CaCO_3$ content of the solid products and the calcite content of $CaCO_3$ in the solid products can be affected by the thickness of the precipitated $CaCO_3$ layers on the $Ca(OH)_2$ surface and by the supersaturation conditions with respect to Ca^{2+} and CO_3^{2-} ions, respectively.

3. Morphology and Particle Sizes of Solid Products

SEM images of the solid products obtained from carbonation tests under different conditions using SC CO_2 combined with the rapid spraying method are shown in Fig. 7. Agglomerates of very small and spherical particles were observed in the solid products obtained from carbonation tests conducted at 35 °C and 7.5 MPa [Fig. 7(a)]. These SEM results are consistent with the FT-RS analysis of the solid products reacted at 35 °C and 7.5 MPa. The small and spherical particles are likely vaterite, which is the predominant $CaCO_3$ polymorph in the solid products obtained under these conditions, as shown in Table 2 and Fig. 6. Rhombohedral calcite was primarily observed in the solid products obtained from carbonation tests conducted at 50 °C and 9.0 MPa [Fig. 7(b)]. In particular, the rhombohedral calcite particles appeared to be more dominant

Table 2. Carbonate polymorph fraction of $CaCO_3$ in solid products obtained from carbonation tests estimated using FT-RS results

Carbonation test conditions			Carbonate polymorph fraction of $CaCO_3$ in solid products		
Temperature (°C)	Pressure (MPa)	Reaction time (h)	Calcite (%)	Aragonite (%)	Vaterite (%)
35	7.5	0.5	16	11	73
		1.0	11	11	78
		2.5	18	12	70
		4.0	15	13	72
50	9.0	0.5	65	13	22
		1.0	87	8	5
		2.5	52	15	33
		4.0	27	19	54
80	12.0	0.5	50	18	32
		1.0	80	9	11
		2.5	69	13	18
		4.0	66	11	23

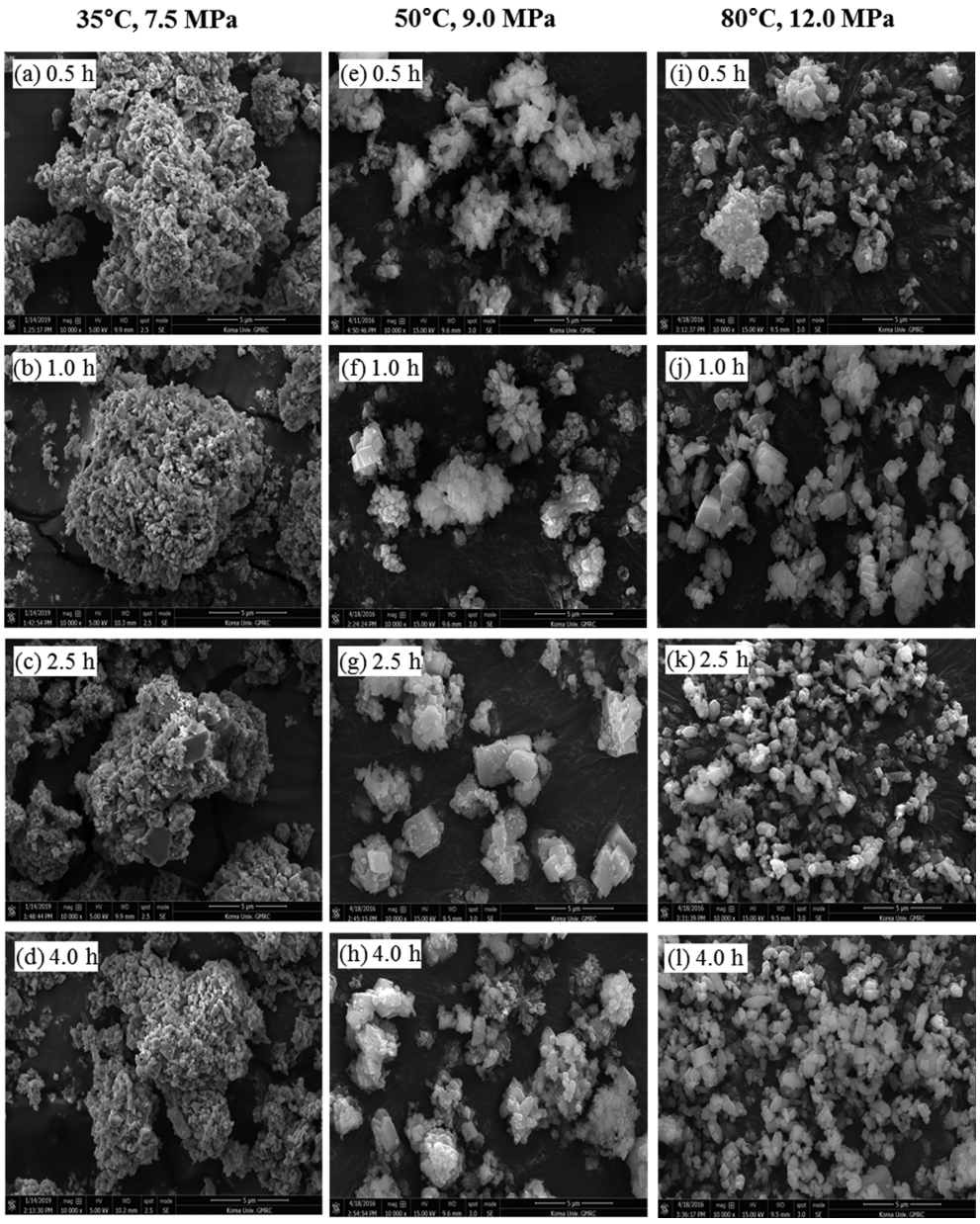

Fig. 7. SEM images of solid products obtained from carbonation tests under conditions of (a)-(d) 35 °C and 7.5 MPa, (e)-(h) 50 °C and 9.0 MPa, and (i)-(l) 80 °C and 12.0 MPa.

in the solid products reacted for 1 h at 50 °C and 9.0 MPa, consistent with the FT-RS analysis results. Rhombohedral calcite and spherical vaterite particles were observed in the solid products obtained from carbonation tests conducted at 80 °C and 12.0 MPa [Fig. 7(c)]. The particle size in the solid products tended to increase with increasing reaction time, irrespective of the test conditions. The 35 °C and 7.5 MPa conditions can cause supersaturation with respect to Ca^{2+} and CO_3^{2-} ions, leading to the predominant precipitation of spherical vaterite. However, in this study, an increase in temperature under high-pressure conditions and a short reaction time could lead to less supersaturation of Ca^{2+} and CO_3^{2-} ions, resulting in the precipitation of predominantly rhombohedral calcite.

The solubility of CO_2 and $Ca(OH)_2$ in water generally decreases with increasing temperature for a given pressure condition. Rhombohedral calcite precipitated at 50 °C and 9.0 MPa, probably because of the low Ca^{2+}/CO_3^{2-} ion ratio. The solubility of $Ca(OH)_2$ and CO_2 in water decreases with increasing temperature; however, the solubility of CO_2 in water increases with increasing pressure. Accordingly, the solubility of $Ca(OH)_2$ in water at 50 °C and 9.0 MPa can be lower than that at 35 °C and 7.5 MPa but higher than that at 80 °C and 12.0 MPa. However, the solubility of CO_2 in water at 50 °C and 9.0 MPa can be higher than that at 35 °C and 7.5 MPa but lower than that at 80 °C and 12.0 MPa. Consequently, the Ca^{2+}/CO_3^{2-} ion ratio at 50 °C and 9.0 MPa is likely low, inducing the precipitation of rhombohedral calcite rather than scalenohedral calcite [6,8].

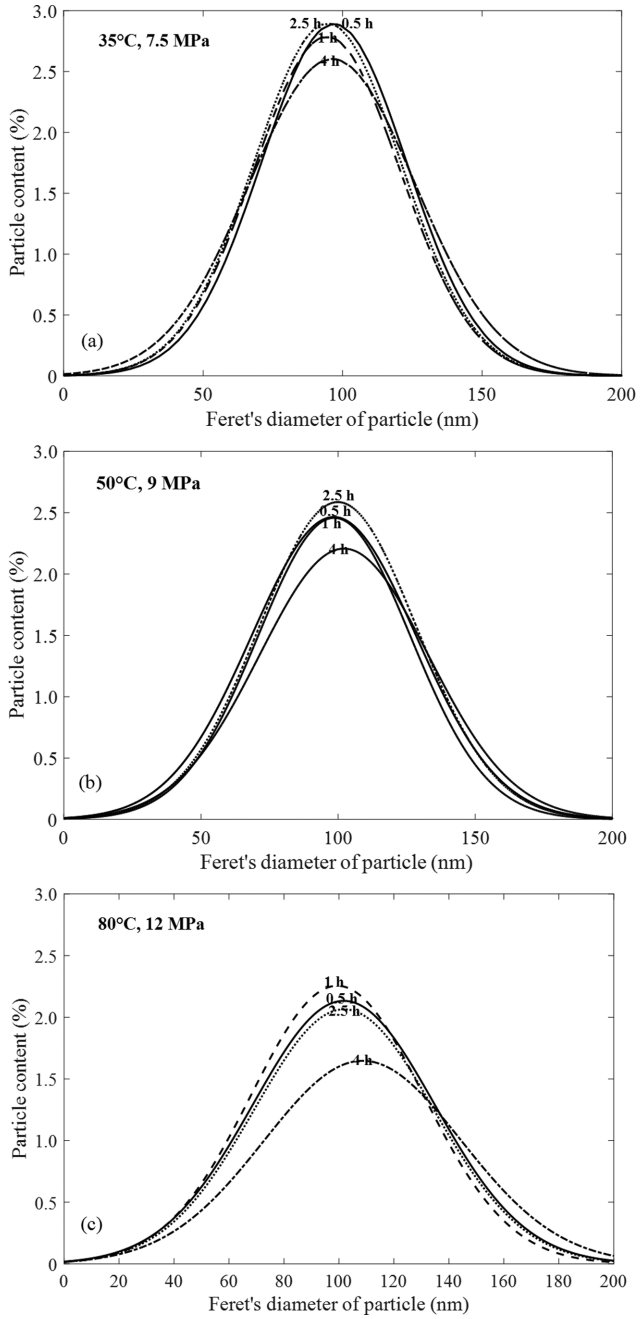

Fig. 8. The particle size distribution (PSD) of solid products obtained from carbonation tests under conditions of (a) 35 °C and 7.5 MPa, (b) 50 °C and 9 MPa, and (c) 80 °C and 12 MPa.

The PSDs of solid products obtained from carbonation tests using SC CO_2 combined with the rapid spraying method under various test conditions were estimated using the Image J software (see Fig. 8). The particle size of solid products ranged between 20 and 180 nm. The PSD curves show a peak at approximately 100 nm, regardless of the test conditions. The peak of the PSD curve was widened and lowered with increasing temperature and pressure (Fig. 8), indicating that particle sizes were relatively well-distributed with increasing temperature and pressure. In addition, the peak of the PSD curve decreased in intensity and shifted towards

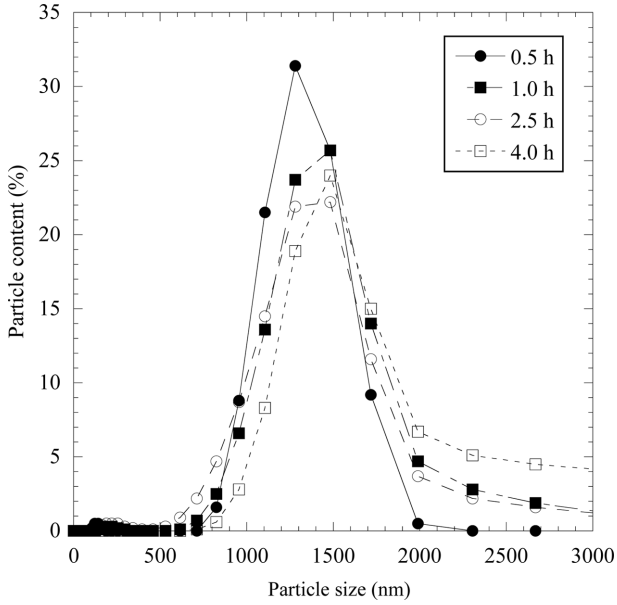

Fig. 9. Particle size distribution (PSD) of the solid product emulsion obtained from carbonation tests at 35 °C and 7.5 MPa.

larger particle sizes with increasing reaction time (Fig. 8), indicating that particle sizes were relatively well-distributed and increased with increasing reaction time. These results collectively suggest that smaller particles can be precipitated at lower temperatures and pressures and with a shorter reaction time.

The PSD curves of the solid products obtained at 35 °C and 7.5 MPa, as determined using a particle size analyzer, are shown in Fig. 9. Particle size analysis was performed using a particle size analyzer for comparison with the PSDs obtained through analysis of the SEM images using the Image J software. Only the solid products obtained at 35 °C and 7.5 MPa were analyzed using a particle size analyzer for comparison, because the amount of solid products available was limited. The particle size of solid products obtained at 35 °C and 7.5 MPa ranged between 800 and 2,000 nm. The peak of the PSD curve corresponds to approximately 1,300-1,500 nm (Fig. 9), which is approximately 13-15 times larger than that obtained by analysis of SEM images using the Image J software (Fig. 8). The larger size of the solid products determined using a particle size analyzer appears to be due to aggregation of the particles in the suspension used for the particle size analysis, even though a dispersion agent was added to disperse the particles in the suspension. However, the shape of the PSD curves was similar to that of the PSD curves obtained through analysis of SEM images using the Image J software (Figs. 8 and 9). In both cases, the peak of the PSD curve was clearly observed to be lowered and shifted towards larger particle sizes with increasing reaction time (Fig. 8), indicating that the particle sizes were relatively well-distributed and increased with increasing reaction time (Fig. 9).

IMPLICATIONS

The extent and rate of $CaCO_3$ conversion in the conventional $CaCO_3$ production processes depend on the extent and rate of dis-

solution of $Ca(OH)_2$ and CO_2 gas in water. $CaCO_3$ initially precipitates on the surface of $Ca(OH)_2$ particles to prevent further $CaCO_3$ formation, resulting in a low extent of $CaCO_3$ conversion [6,7]. SC CO_2 has been proposed as a reactant to enhance the extent and rate of $CaCO_3$ production because SC CO_2 can cause very high CO_2 partial pressures, resulting in an increase in the amount of CO_2 dissolved in water [9,12]. However, the carbonation method with SC CO_2 still has problems with respect to $CaCO_3$ precipitation on the $Ca(OH)_2$ surface. The carbonation of a $Ca(OH)_2$ slurry using SC CO_2 in combination with ultrasonic agitation has been proposed to reduce the effect of $CaCO_3$ precipitation on the $Ca(OH)_2$ surface [7,13].

On the basis of the results of the present study, the rapid spraying method can produce the same effect as ultrasonic agitation, reducing the effect of $CaCO_3$ precipitation on the $Ca(OH)_2$ surface for the carbonation of $Ca(OH)_2$-H_2O-SC CO_2. In the case of carbonation in $Ca(OH)_2$-H_2O slurry with SC CO_2 combined with the rapid spraying method, the exfoliation of initially precipitated $CaCO_3$ layers on the $Ca(OH)_2$ surface or particle destruction, which can expose the reactive surface, can occur during rapid depressurization when the mixture is sprayed into a plastic container through a very small-diameter tube within a very short period (~5 s). The exfoliation or particle destruction can enhance the extent and rate of $CaCO_3$ conversion by exposing reactive Ca^{2+} ions to CO_3^{2-} ions.

In addition, the size and shape of the $CaCO_3$ can be controlled through manipulation of the test conditions (temperature, pressure, and reaction time). Because the degree of crystal growth depends on the reaction time, a shorter reaction time results in smaller particles. The solubility of $Ca(OH)_2$ and CO_2 in water decreases with increasing temperature; however, the solubility of CO_2 in water at intermediate temperature and pressure conditions (50 °C and 9.0 MPa) increases with increasing pressure. The effect of temperature on the solubility of $Ca(OH)_2$ and CO_2 can be offset by the effect of pressure, resulting in a low Ca^{2+}/CO_3^{2-} ion ratio. A low Ca^{2+}/CO_3^{2-} ion ratio causes precipitation of rhombohedral calcite rather than scalenohedral calcite at 50 °C and 9.0 MPa.

CONCLUSIONS

The carbonation of $Ca(OH)_2$-H_2O slurry with SC CO_2 using the rapid spraying method can enhance the extent and rate of $CaCO_3$ conversion compared with conventional carbonation methods with SC CO_2, likely because mass transfer through the initially precipitated $CaCO_3$ layers on the $Ca(OH)_2$ surface is promoted. The effect of very rapid spraying, which causes rapid depressurization, on the exfoliation of precipitated $CaCO_3$ layers on the $Ca(OH)_2$ surface is similar to that of ultrasonic agitation. The carbonation with SC CO_2 using the rapid spraying method under conditions of low temperature and low pressure (35 °C and 7.5 MPa) can produce $CaCO_3$ composed mostly of spherical vaterite (70-78%). The conditions under which the $CaCO_3$ conversion and calcite content were maximal were 50 °C, 9.0 MPa, and 1 h of reaction time ($CaCO_3$ conversion: 93%; calcite content of $CaCO_3$: 87%).

These experimental results suggest that the proposed carbonation technique for $Ca(OH)_2$-H_2O-SC CO_2 using the rapid spraying method can be used to promote the $CaCO_3$ conversion rate and reduce the effect of $CaCO_3$ layers precipitated on the $Ca(OH)_2$ surface on the extent of $CaCO_3$ conversion. Carbonation tests with SC CO_2 using rapid spraying under three different sets of temperature and pressure conditions were conducted to determine the appropriate experimental conditions; the optimal conditions (50 °C, 9.0 MPa, and 1 h) were then proposed. However, controlling the size, shape, and polymorphism of the solid products obtained by carbonation using the rapid spraying method is difficult. Therefore, further studies are needed to confirm the optimal experimental conditions and to investigate the effect of test conditions (e.g., temperature, pressure, reaction time, depressurization rate, and nozzle size) on both the $CaCO_3$ conversion efficiency and the size and shape of the carbonates.

ACKNOWLEDGEMENTS

This research was supported by the National Research Foundation (NRF-2017R1A2B4008238) of the Ministry of Science, ICT & Future Planning, Korea. This work was partly supported by Korea Environment Industry & Technology Institute (KEITI) through Subsurface Environment Management (SEM) Project, funded by Korea Ministry of Environment.

REFERENCES

1. O. Söhnel and J. W. Mullin, *J. Cryst. Growth*, **60**, 239 (1982).
2. N. H. Leeuw and S. C. Parker, *J. Phys. Chem.*, **102**, 2914 (1998).
3. F. Lippmann, *Sedimentary carbonate minerals*, Springer Science & Business Media, Berlin (1973).
4. S. R. Dickinson, G. E. Henderson and K. M. McGrath, *J. Cryst. Growth*, **244**, 369 (2002).
5. D. J. Hwang, J. Y. Ryu, Y. H. Yu, K. H. Cho, J. W. Ahn and C. Han, *J. Ind. Eng. Chem.*, **20**, 2727 (2014).
6. C. Domingo, E. Loste, J. Gomez-Morales and J. Garcia-Carmona, J. Fraile, *J. Supercrit. Fluids*, **36**, 202 (2006).
7. A. M. López-Periago, R. Pacciani, C. García-Gonzalez, L. F. Vega and C. Domingo, *J. Supercrit. Fluids*, **52**, 298 (2010).
8. W. Gu, D. W. Bousfield and C. P. Tripp, *J. Mater. Chem.*, **16**, 3312 (2006).
9. G. Montes-Hernandez, F. Renard, N. Geoffroy, L. Charlet and J. Pironon, *J. Cryst. Growth*, **308**, 228 (2007).
10. J. Li and E. G. Azevedo, *Recent. Pat. Chem. Eng.*, **1**, 157 (2008).
11. D. Lozowski, *Chem. Eng.*, **117**, 15 (2010).
12. O. Regnault, V. Lagneau and H. Schneider, *Chem. Geol.*, **265**, 113 (2009).
13. A. M. López-Periago, R. Pacciani, C. García-Gonzalez, L. F. Vega and C. Domingo, *Cryst. Growth Des.*, **52**, 298 (2011).
14. P. Hawae, N. Chusri, P. Sumanatrakul and C. Siripatana, *PACCON2015* (2015).
15. M. Mchugh and V. Krukonis, *Supercritical fluid extraction: principles and practice*, Butterworth, Stoneham (1986).
16. P. G. Debenedetti, *AIChE J.*, **36**, 1289 (1990).
17. I. Pane and W. Hansen, *Cem. Concr. Res.*, **35**, 1155 (2005).
18. C. G. Kontoyannis and N. V. Vagenas, *Analyst*, **125**, 251 (2000).
19. Z. G. Wu, J. Wang, Y. Guo and Y. R. Jia, *Cryst. Res. Technol.*, **53**, 1700120 (2018).

20. J. Chen and L. Xiang, *Powder Technol.*, **189**, 64 (2009).
21. A. Niedermayr, S. J. Köhler and M. Dietzel, *Chem. Geol.*, **340**, 105 (2013).
22. D. H. Chu, M. Vinoba, M. Bhagiyalakshmi, I. H. Baek, S. C. Nam, Y. Yoon, S. H. Kim and S. K. Jeong, *RSC Adv.*, **3**, 21722 (2013).
23. T. Zhao, B. Guo, F. Zhang, F. Sha, Q. Li and J. Zhang, *ACS Appl. Mater. Interfaces*, **7**, 15918 (2015).
24. D. Konopacka-Łyskawa, B. Kościelska and J. Karczewski, *Mater. Chem. Phys.*, **192**, 13 (2017).
25. J. Jiang, Y. Wu, C. Chen, X. Wang, H. Zhao, S. Xu, C. C. Yang and B. Xiao, *Adv. Powder Technol.*, **29**, 2416 (2018).
26. Y. Ding, Y. Liu, Y. Ren, H. Yan, M. Wang, D. Wang, X. Y. Lu, B. Wang, T. Fan and H. Guo, *Powder Technol.*, **333**, 410 (2018).
27. Z. G. Wu, J. Wang, Y. Guo and Y. R. Jia, *Cryst. Res. Technol.*, **53**, 1700120 (2018).
28. J. Zhang, C. Zhao, A. Zhou, C. Yang, L. Zhao and Z. Li, *Constr. Build. Mater.*, **224**, 815 (2019).
29. W. Pabst and E. Gregorová, *ICP Prague 2007* (2007).
30. H. G. Merkus, *Particle size measurements: fundamentals, practice, quality*, Springer, Berlin (2012).
31. S. Goto, K. Suenaga, T. Kado and M. Fukuhara, *J. Am. Ceram. Soc.*, **78**, 2867 (1995).
32. K. Vance, G. Falzone, I. Pignatelli, M. Bauchy, M. Balonis and G. Sant, *Ind. Eng. Chem. Res.*, **54**, 8908 (2015).
33. Z. V. Padanyi, *Solid State Commun.*, **8**, 541 (1970).
34. J. Harris, I. Mey, M. Hajir, M. Mondeshki and S. E. Wolf, *Cryst. Eng. Comm.*, **17**, 36 (2015).
35. N. Spanos and P. G. Koutsoukos, *J. Cryst. Growth*, **191**, 783 (1998).
36. Y. S. Han, G. Hadiko, M. Fuji and M. Takahashi, *J. Cryst. Growth*, **276**, 541 (2005).